

RESEARCH ARTICLE

Stabilization of Infinitesimally Rigid Formations of Multi-Robot Networks

Laura Krick^a, Mireille E. Broucke^{a*}, and Bruce A. Francis^a

^a*Edward S. Rogers Sr. Department of Electrical and Computer Engineering, University of Toronto,
Toronto, ON M5S 3G4, Canada;*

(June 18, 2008)

This paper considers the design of a formation control for multivehicle systems that uses only local information. The control is derived from a potential function based on an undirected infinitesimally rigid graph that specifies the target formation. A potential function is obtained from the graph, from which a gradient control is derived. Under this controller the target formation becomes a manifold of equilibria for the multivehicle system. It is shown that infinitesimal rigidity is a sufficient condition for local asymptotical stability of the equilibrium manifold. A complete study of the stability of the regular polygon formation is presented and results for directed graphs are presented as well. Finally, the controller is validated experimentally.

Keywords: Cooperative control, multiagent formations, graph rigidity.

1 Introduction

This paper considers distributed control of systems of agents that are interconnected dynamically or have a common objective, and where control is local, with the possible exception of high-level intermittent centralized supervision. Undoubtedly these kinds of systems will become more and more prevalent as embedded hardware evolves. An interesting example and area of ongoing research is the control of a group of autonomous mobile robots, ideally without centralized control or a global coordinate system, so that they work cooperatively to accomplish a common goal. The aims of such research are to achieve systems that are scalable, modular, and robust. These goals are similar to those of sensor networks—networks of inexpensive devices with computing, communications, and sensing capabilities. Such devices are currently commercially available and include products like the Intel Mote. A natural extension of sensor networks would be to add simple actuators to the sensors to make them mobile, and then to adapt the network configuration to optimize network coverage.

If global coordinates are known and there is an omniscient supervisor, these problems are routine: Each robot could be stabilized to its assigned location. The current technology to provide global coordinates is the Global Positioning System (GPS). However, the use of GPS for position information in multi-agent applications has several problems: The precision of GPS depends on the number of satellites currently visible; during periods of dense cloud cover, in urban areas, and under dense vegetation, there may be no line of sight between the receiver and the GPS satellite. These problems in obtaining global coordinates make it natural to study decentralized control.

The simplest problem is stabilizing the robots to a common location, frequently called the *rendezvous problem*. Many different techniques have been used to solve this problem, for example, cyclic pursuit (Marshall et al. 2004) and the circumcentre law (Cortés et al. 2004). The solution in Lin et al. (2004) involves asynchronous stop-and-go cycles. Goldenberg et al. (2004) considers

*Corresponding author. Email: broucke@control.utoronto.ca
ISSN: 0020-7179 print/ISSN 1366-5820 online
© 200x Taylor & Francis
DOI: 10.1080/0020717YYxxxxxxx
<http://www.informaworld.com>

a problem of decentralized, self organizing communication nodes with mobility. In this case, the mobility is used to improve communication performance. Another possible goal for mobile sensor networks is to optimize sensor placement by minimizing a cost function. This type of problem is studied in Cortés et al. (2004).

An interesting approach to formation control is that of Olfati-Saber (2006). The robots are point masses (double integrators) with limited vision, and he proposes using rigid graph theory to define the formation; he also proposes a gradient control law involving prescribed distances. The limitation is that the network is not homogeneous—special so-called γ -agents are required to achieve flocking.

Finally Smith et al. (2006) considers the problem of achieving polygon formations without global coordinates, but the solution is complete only for three robots.

The starting point for our paper is Olfati-Saber and Murray (2002). Following that paper, we use graphs to define formations, but instead of global rigidity we use infinitesimal rigidity and instead of the double integrator model we use the simpler single integrator (kinematic point). More substantially, our stability analysis is complete whereas, being a conference paper, Olfati-Saber and Murray (2002) provides only a sketch. In particular, Olfati-Saber and Murray (2002) has no topological analysis of the equilibrium set and does not note that the equilibrium set is not compact. Moreover, Olfati-Saber and Murray (2002) uses a LaSalle argument to prove stability, but since the equilibrium set is not compact, this is open to question. Furthermore, Olfati-Saber and Murray (2002) does not address if the trajectories have a limit on the equilibrium set. Additional, more technical remarks follow in Remark 2.

The first contribution of the paper is a decentralized gradient control law to stabilize a group of point mass robots to any formation corresponding to an infinitesimally rigid framework. A complete stability analysis is provided in Section 5. Regular polygon formations are studied in Section 6, where it is shown that the conditions of our theory can be applied to this case. A drawback of the proposed controller is that it requires two-way communication between robots: if robot i can sense robot j , then robot j can sense robot i . In Section 7 we address the formation stabilization problem under the constraint that, instead, the sensor graph is directed. It is shown that when the formation graph is constructed using a Henneberg insertion procedure to achieve an infinitesimally rigid framework, the foregoing stability analysis for undirected graphs still applies.

Before presenting the main results in Sections 5, 6, and 7, we first give an overview of concepts from graph theory and particularly graph rigidity theory in Section 2. In Section 3 the stabilization problem is formulated and in Section 4 the gradient control law is proposed and some of its properties are analyzed.

2 Background

2.1 Notation

We denote the Jacobian of a function $f : \mathbb{R}^n \rightarrow \mathbb{R}^m$ evaluated at a point x as $J_f(x)$. In the special case when $f : \mathbb{R}^n \rightarrow \mathbb{R}$, the Jacobian of f is the gradient of f and we denote it by $\nabla f(x)$. Occasionally for convenience during calculations of the Jacobian, the notation $\frac{\partial}{\partial x}$ will be used to represent $J_f(x) = \frac{\partial}{\partial x} f(x)$.

2.2 Graph Theory

A directed graph $G = (V, E)$ is a pair consisting of a finite set of vertices $V := \{1, \dots, n\}$ and a set of edges $E \subset V \times V$. We assume the edges are ordered; that is $E = \{1, \dots, m\}$, where $m \in \{1, \dots, n(n-1)\}$. We exclude the possibility of self loops. An undirected graph is a directed graph such that if there is an edge e_i from vertex j to vertex k , then there is also an edge e_l from vertex k to vertex j . For undirected graphs, we omit the arrows in the pictorial representation

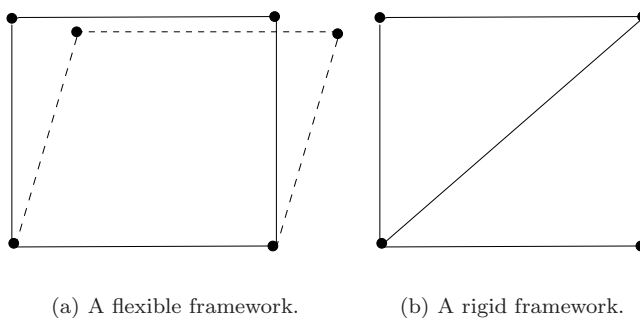


Figure 1.

of the graph. A special undirected graph is the graph K_n , the *complete graph* with n vertices, which has an edge between every pair of vertices. A useful matrix associated with a graph G is the $m \times n$ *incidence matrix*, H . It is determined by the edges e_i of G : row i of H is determined by e_i and has two non-zero entries: a 1 in column k and a -1 in column j , where e_i is the edge between vertex j and vertex k . Thus, by definition, $H\mathbf{1} = 0$, where $\mathbf{1}$ is the vector with a 1 in each component.

Lemma 2.1: (Biggs (1974), p. 23) *The incidence matrix H has rank $n - c$ where c is the number of connected components of G .*

For the remainder of this work we assume that all graphs are connected and thus $\text{Ker}(H)$ is one dimensional. Also, directed graphs are considered connected if the corresponding undirected graph is connected.

2.3 Graph Rigidity

To introduce the notion of rigidity of graphs we must view a graph as a framework embedded in the plane, \mathbb{R}^2 . Let $G = (V, E)$ be an undirected graph with n vertices. We embed G into \mathbb{R}^2 by assigning to each vertex i a location $p_i \in \mathbb{R}^2$. Define the composite vector $p = (p_1, \dots, p_n) \in \mathbb{R}^{2n}$. A *framework* is a pair (G, p) .

We define the *rigidity function* associated with the framework (G, p) as the function $g_G : \mathbb{R}^{2n} \rightarrow \mathbb{R}^{|E|}$ given by

$$g_G(p) := (\dots, \|p_k - p_j\|^2, \dots),$$

The i th component of $g_G(p)$, $\|p_k - p_j\|^2$, corresponds to the edge e_i in E , where vertices j and k are connected by e_i . Note that this function is not unique and depends on the ordering given to the edges.

2.3.1 Rigidity and Global Rigidity

There are several equivalent definitions of rigidity. The definitions below are taken from Asimow and Roth (1979).

Definition 2.2 A framework (G, p) is *rigid* if there exists a neighbourhood $\mathcal{U} \subset \mathbb{R}^{2n}$ of p such that $g_G^{-1}(g_G(p)) \cap \mathcal{U} = g_K^{-1}(g_K(p)) \cap \mathcal{U}$, where K is the complete graph with the same vertices as G .

It is also possible to define a global version of rigidity.

Definition 2.3 A framework (G, p) is *globally rigid* if $g_G^{-1}(g_G(p)) = g_K^{-1}(g_K(p))$.

The level set $g_G^{-1}(g_G(p))$ consists of all possible points that have the same edge lengths as

4
t

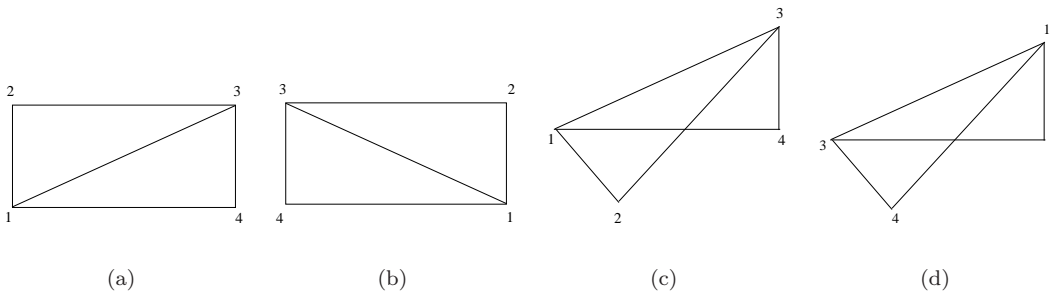


Figure 2. Possible embeddings of a graph with four vertices.

the framework (G, p) . For the complete graph K the set $g_K^{-1}(g_K(p))$ consists of points related by rotations and translations, i.e., rigid body motions, of the framework (K, p) . We conclude that a graph G is rigid if the level set $g_G^{-1}(g_G(p))$ in a neighbourhood of p contains only points corresponding to rotations and translations of the formation at p . For example, consider the framework in Figure 1(a). It is possible to translate the top two points of the framework while maintaining the four edge lengths to obtain a graph that is not isomorphic to the original graph; the lengths of the diagonals change, so the framework is not rigid. If we add one more edge to the framework we obtain the framework in Figure 1(b). For this framework, every perturbation of the vertices that maintains the edge lengths is isomorphic to the original framework, so this graph is rigid.

To illustrate the difference between rigidity and global rigidity consider the example of a graph with four vertices and

$$g_G(z) = \begin{bmatrix} \|z_1 - z_2\|^2 \\ \|z_2 - z_3\|^2 \\ \|z_3 - z_4\|^2 \\ \|z_4 - z_1\|^2 \\ \|z_3 - z_1\|^2 \end{bmatrix} \text{ and } d = \begin{bmatrix} 1 \\ 2^2 \\ 1 \\ 2^2 \\ 5 \end{bmatrix}. \tag{1}$$

There are four possible distinct frameworks for this graph, as shown in Figure 2. Each of these frameworks is rigid, but not globally rigid, since solutions z of $g_G(z) = d$ can correspond to either of two different complete graphs (when part of the graph is flipped over). Instead, if the graph were also globally rigid, then $g_G(z) = d$ would have solutions corresponding to only one complete graph and only two distinct embeddings. These two embeddings would be reflections of one another. Figure 3 illustrates this case.

2.3.2 Infinitesimal Rigidity

We refer to the matrix $J_{g_G}(p)$ as the *rigidity matrix* of (G, p) . The rigidity matrix is useful in defining some other concepts related to graph rigidity. (Note that we consider graphs with at least two vertices; otherwise the concepts introduced here will not be well-defined).

Definition 2.4 A point p is a *regular point* of the graph G with n vertices if

$$\text{rank} J_{g_G}(p) = \max \{ \text{rank} J_{g_G}(q) \mid q \in \mathbb{R}^{2n} \}.$$

In Figure 4(a) we see that the graph K_3 is embedded at a regular point. Instead, Figure 4(b) shows the graph K_3 embedded at a point that is not regular.

The idea of infinitesimal rigidity is to allow the vertices to move infinitesimally, while keeping the rigidity function constant up to first order. Let δp be an infinitesimal motion of the framework

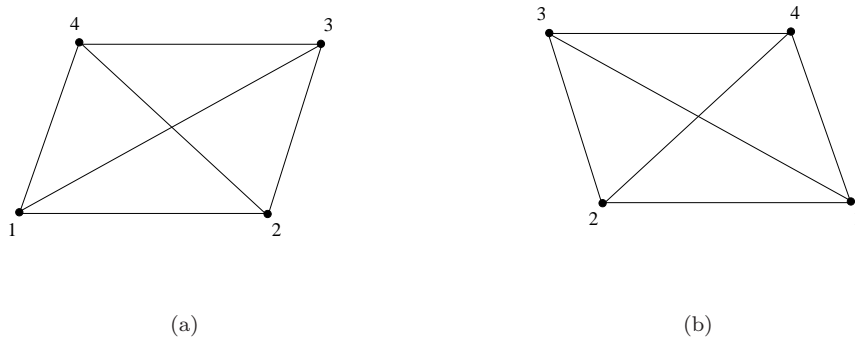


Figure 3. The two possible embeddings of the graph K_4 . Note that Figure 3(a) is a reflection of Figure 3(b).

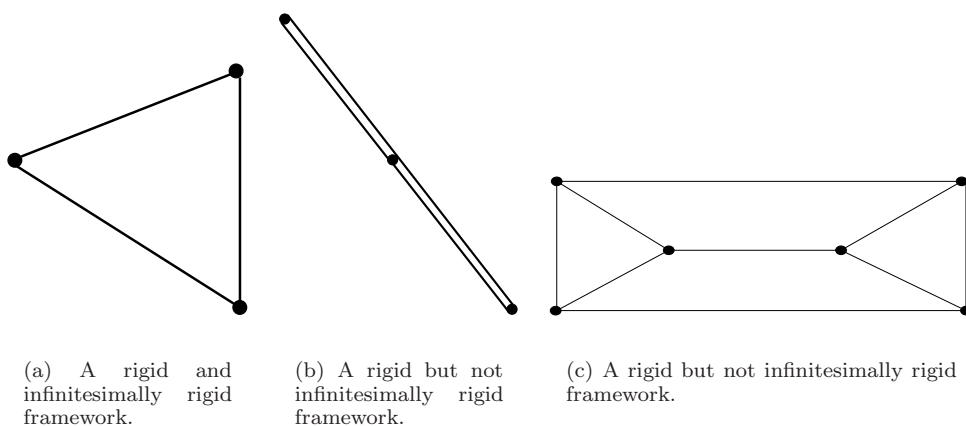


Figure 4.

(G, p) . Then the Taylor series expansion of g_G about p is

$$g_G(p + \delta p) = g_G(p) + J_{g_G}(p)\delta p + \text{higher order terms.}$$

The rigidity function remains constant up to first order when $J_{g_G}(p)\delta p = 0$, that is, when δp belongs to $\text{Ker} J_{g_G}(p)$. The dimension of this kernel is at least 3 because $g_G(p)$ will not change if p is perturbed by a rigid body motion. Infinitesimal rigidity is when the dimension of the kernel is not larger than 3.

Definition 2.5 (Asimow and Roth (1979)) A framework (G, p) is *infinitesimally rigid* in the plane if $\dim(\text{Ker} J_{g_G}(p)) = 3$, or equivalently if

$$\text{rank} J_{g_G}(p) = 2n - 3.$$

If a framework is infinitesimally rigid, then it is also rigid. The converse is not true. The following theorem outlines when rigidity and infinitesimal rigidity are equivalent.

Theorem 2.6 : (Asimow and Roth (1979)) A framework (G, p) is *infinitesimally rigid* if and only if (G, p) is rigid and p is a regular point.

Observe that for a graph to be infinitesimally rigid in the plane it must have at least $2n - 3$ edges. If it has exactly $2n - 3$ edges, we say that the graph is *minimally rigid*.

The two different embeddings of K_3 shown in Figure 4(a)-(b) illustrate some of the rigidity properties. Both frameworks shown are embeddings of the complete graph. They are both rigid and globally rigid. The framework shown in Figure 4(a) is also infinitesimally rigid. If we check the rigidity matrix for any point p where the vertices are not collinear we will find it has rank 3. The framework in Figure 4(b) is not infinitesimally rigid. We can check this using the rigidity matrix. Let the embedding of the points in the plane be $z_1 = (0, 0)$, $z_2 = (0, 1)$, $z_3 = (0, 2)$. The rigidity function for this graph is

$$g_G(z) = \begin{bmatrix} \|z_1 - z_2\|^2 \\ \|z_2 - z_3\|^2 \\ \|z_3 - z_1\|^2 \end{bmatrix}.$$

Then

$$J_{g_G}(p) = 2 \begin{bmatrix} z_1^T - z_2^T & z_2^T - z_1^T & 0 \\ 0 & z_2^T - z_3^T & z_3^T - z_2^T \\ z_1^T - z_3^T & 0 & z_3^T - z_1^T \end{bmatrix}.$$

If we check the rank at a collinear point p we obtain $\text{rank } J_{g_G}(p) = 2 < 2n - 3$. As the rigidity matrix does not have maximal rank, p is not a regular point; consistent with Theorem 2.6, a rigid framework is not infinitesimally rigid at a non-regular point.

Typically, frameworks that are rigid but fail to be infinitesimally rigid have collinear or parallel edges. For instance the graph in Figure 4(c) is rigid but not infinitesimally rigid because the framework could undergo an infinitesimal distortion by perturbing the top link horizontally; the two triangles would then rotate infinitesimally, and the middle link rotate infinitesimally.

2.3.3 Constructing Rigid Graphs

Any collection of n points in the plane can be connected to form a rigid framework. For instance, we can connect the points using K_n , the complete graph. In subsequent sections we will find that the complexity of the control is proportional to the number of edges in a certain graph. Using the complete graph will result in a design that is not scalable: as the number of connections needed for n vertices is $\frac{n^2-n}{2}$. Instead, from the definition of infinitesimal rigidity, we see a graph can be infinitesimally rigid with only $2n - 3$ edges. For $n > 3$, this is fewer edges than the complete graph.

A rigid graph can be constructed for any embedding of n vertices in the plane in the following manner. First, number all the vertices. Next, add an edge between vertex 1 and vertex 2. If we consider the framework formed by vertex 1 and vertex 2, we see that it is the complete graph, and thus is rigid. The remaining vertices are added in order to the connected component of the graph, connecting each one to the previously connected graph structure by two edges. This operation is sometimes referred to as a *Henneberg insertion*, Berge (2005). This type of insertion preserves graph rigidity because each vertex has two degrees of freedom. By connecting the vertex to the previously connected graph structure by two edges the position of the vertex is subject to two constraints, removing both degrees of freedom. This procedure results in a framework that is not only rigid but also minimally rigid; that is, if we remove any edge the framework is no longer rigid.

3 Problem Formulation

Consider n robots in the plane, \mathbb{R}^2 . The robots are wheeled vehicles with sensors that allow them to measure the relative positions of some of the other vehicles. Such data can be obtained using a camera or a radar system. The simplest model for a wheeled vehicle is the kinematic unicycle. To simplify the analysis, using a standard procedure we assume the unicycle model has been

feedback linearized about a point some distance in front of each unicycle. The robots then have a point kinematic model given by the differential equation

$$\dot{z}_i = u_i, \quad i \in \{1, \dots, n\} \quad (2)$$

where $z_i = (x_i, y_i) \in \mathbb{R}^2$ is the location of the i th robot in the plane and $u_i \in \mathbb{R}^2$ is the control input for the i th robot. We define the composite state vector $z = (z_1, \dots, z_n)$, as a vector in $(\mathbb{R}^2)^n$.

The *target formation* is described by a pair $\{G, d\}$ where G is an undirected graph whose vertices represent the robots, and vector $d \in \mathbb{R}^m$ specifies m target lengths for the edges. We refer to G as the *formation graph*. The robots achieve the target formation when the length of edge i is the prescribed distance $d_i > 0$.

Associated with the formation control problem is also a *sensor graph* that describes the sensor data seen by each robot in the closed-loop system. The sensor graph is a directed graph with each robot represented as a vertex in the graph. Given a controller u , if u_i is a function of z_j , then the sensor graph will have an edge from vertex i to vertex j . Also, we require that the control be a function only of relative measurements. For example if robot 1 can see robots 3 and 5, then the measurements available to robot 1 are $z_3 - z_1$ and $z_5 - z_1$, and u_1 can be a function of these two measurements. We refer to this as a *distributed control law*. We have the following problem.

Problem 3.1 Given the system (2) and a target formation $\{G, d\}$ such that $g_G^{-1}(d) \neq \emptyset$ and such that the framework (G, p) is infinitesimally rigid at each $p \in g_G^{-1}(d)$, design a distributed control law u whose sensor graph is G with the following two properties: (1) every $p \in g_G^{-1}(d)$ is a stable equilibrium of the closed-loop system, and (2) for every initial condition in a neighborhood of $g_G^{-1}(d)$, the closed-loop trajectory tends to a unique equilibrium point in $g_G^{-1}(d)$.

4 Gradient Control

In this section we propose a controller to solve Problem 3.1. We start with the framework (G, p) . It has certain edges joining certain vertices. Using exactly the same link structure, define relative positions between robot positions, that is, define $e_i = z_k - z_j$, where p_k, p_j are linked on the framework. Without loss of generality $j < k$. Notice that e_i is an error vector in the direction of edge i and $\|e_i\|^2$ is the i th term in the rigidity function, $g_G(z)$.¹ We also form the composite vector $e = (e_1, \dots, e_m) \in \mathbb{R}^{2m}$. This vector is a linear function of z via the incidence matrix, $H \in \mathbb{R}^{m \times n}$, of the graph G ; namely, with the definition

$$\hat{H} := H \otimes I_2 \in \mathbb{R}^{2m \times 2n}, \quad (3)$$

we have

$$e = \hat{H}z. \quad (4)$$

For example, for the complete graph K_3

$$H = \begin{bmatrix} 1 & -1 & 0 \\ 0 & 1 & -1 \\ 1 & 0 & -1 \end{bmatrix}, \quad \hat{H} = \begin{bmatrix} I_2 & -I_2 & 0 \\ 0 & I_2 & -I_2 \\ I_2 & 0 & -I_2 \end{bmatrix}.$$

¹The notation e_i is used to refer both to the edge i and as an error vector pointing in the direction of edge i in the framework.

4.1 Special Case: The Rendezvous Problem

The rendezvous problem is the special case of the formation stabilization problem where $d = 0$. If L denotes the Laplacian of the graph G , and $\hat{L} = L \otimes I_2$, a linear solution to this problem is to let $u = -\hat{L}z$, and then

$$\dot{z} = -\hat{L}z. \quad (5)$$

If G is connected, then 0 is a simple eigenvalue of L (Frobenius' theorem) and rendezvous follows. Recall that if G is undirected, the Laplacian is a symmetric matrix. Furthermore, the Laplacian and incidence matrices are related by $\hat{L} = \hat{H}^T \hat{H}$ (Proposition 4.8 in Biggs (1974)). Thus

$$\hat{L}z = \left[\nabla \left(\frac{1}{2} \|\hat{H}z\|^2 \right) \right]^T.$$

The function $\frac{1}{2} \|\hat{H}z\|^2$ is positive semidefinite. So the control law in (5) is not only a gradient control law, as all symmetric linear controls are, but a gradient control law for a positive semidefinite potential function. This suggests considering a gradient control of a positive semidefinite potential function for the general formation stabilization problem.

4.2 Control Law

We now consider a gradient control law to maintain an arbitrary formation of robots. First we define a vector norm function $v : \mathbb{R}^{2m} \rightarrow \mathbb{R}^m$:

$$v(e) = (\|e_1\|^2, \dots, \|e_m\|^2).$$

Then using (4) we define $g : \mathbb{R}^{2n} \rightarrow \mathbb{R}^m$ by

$$g(z) := v(e) = v(\hat{H}z). \quad (6)$$

Notice that $g(z)$ is precisely the rigidity function $g_G(z)$ (henceforth the subscript is dropped).

As a candidate potential function, we consider the positive definite function of $g(z) - d$

$$\phi(z) = \frac{1}{2} \|g(z) - d\|^2. \quad (7)$$

Note that $\phi(z)$ is a positive semidefinite function of z and $\phi(z) = 0$ if and only if $g(z) = d$. We propose the gradient control

$$u = -(\nabla \phi(z))^T.$$

It follows from (2) and applying the chain rule to (7) that

$$\begin{aligned} \dot{z} &= -(J_g(z))^T (g(z) - d) \\ &= -\hat{H}^T J_v(\hat{H}z)^T (v(\hat{H}z) - d) \\ &= -\hat{H}^T J_v(e)^T (v(e) - d), \end{aligned} \quad (8)$$

where the Jacobian of v is

$$J_v(e) = 2 \begin{bmatrix} e_1^T & \dots & 0 \\ \vdots & \ddots & \vdots \\ 0 & \dots & e_m^T \end{bmatrix}. \quad (9)$$

It is evident that the control is a function only of the relative measurements, as required by the problem specification. More specifically, the control law for each robot is

$$\dot{z}_i = u_i = - \sum_{j \in \{\text{edges leaving } i\}} \frac{1}{2} (\|e_j\|^2 - d_j) e_j, \quad (10)$$

consistent with the problem specification that the sensor graph be identically the same as the formation graph. In the following lemma we list further interesting properties of the controlled system (8). Proofs are omitted since the results are easily verified.

Lemma 4.1:

- (1) The centroid $z^\circ := \frac{1}{n} \sum_{i=1}^n z_i$ is stationary: $\dot{z}^\circ = 0$.
- (2) The control in (8) is independent of the system of global coordinates; that is, for every $w \in \mathbb{R}^2$,

$$\nabla \phi(z + \mathbf{1} \otimes w) = \nabla \phi(z),$$

and for every orthogonal matrix $R \in \mathbb{R}^{2 \times 2}$,

$$\nabla \phi(z) \hat{R}^T = \nabla \phi(\hat{R}z),$$

where $\hat{R} = I_n \otimes R$.

- (3) Define the collinear set $\mathcal{C} := \{z \in \mathbb{R}^{2n} \mid (\exists w \in \mathbb{R}^2)(\forall i) (z_i - z^\circ) \in \text{span}(w)\}$. Then \mathcal{C} is invariant under (8).

4.3 Coordinate Transformation

In this section we perform a coordinate transformation that separates the centroid dynamics from the remaining dynamics of the system. This will be particularly helpful in several of the analyses that follow.

Let P be an orthonormal matrix whose first two rows are $\frac{1}{n} \mathbf{1}^T \otimes I_2$. Then consider the transformation

$$\tilde{z} = \begin{bmatrix} z^\circ \\ \bar{z} \end{bmatrix} = Pz,$$

where z° is the centroid of z , as discussed in Lemma 4.1. Define

$$\tilde{H} = \hat{H}P^{-1}. \quad (11)$$

From the definition of \tilde{H} it is clear that $\tilde{H}\tilde{z} = \hat{H}z$. We now solve for the \tilde{z} dynamics, obtaining

$$\begin{aligned} \dot{\tilde{z}} &= P\dot{z} \\ &= -\tilde{H}^T \left(J_v(\tilde{H}\tilde{z}) \right)^T (v(\tilde{H}\tilde{z}) - d). \end{aligned} \quad (12)$$

So, $\dot{\tilde{z}} = -[\nabla\tilde{\phi}(\tilde{z})]^T$, where $\tilde{\phi}(\tilde{z}) = \frac{1}{2}\|v(\tilde{H}\tilde{z}) - d\|^2$.

Next we consider an interesting property of \tilde{H} . Note that since the first two columns of P^{-1} are in $\text{Ker}(\hat{H})$, \tilde{H} has the form $\begin{bmatrix} 0 & \overline{H} \end{bmatrix}$. From Lemma 2.1, $\dim(\text{Ker}(H)) = 1$, so $\dim(\text{Ker}(\hat{H})) = 2$. Then by using the dimension of $\text{Ker}(\hat{H})$, the invertibility of P , and the block form of \tilde{H} , we know that $\text{Ker}(\overline{H}) = \{0\}$.

Now expand $\tilde{H}\tilde{z}$:

$$\tilde{H}\tilde{z} = \begin{bmatrix} 0 & \overline{H} \end{bmatrix} \begin{bmatrix} z^\circ \\ \bar{z} \end{bmatrix} = \overline{H}\bar{z}. \tag{13}$$

So the \tilde{z} dynamics from (12) can be rewritten using (11) and (13) as

$$\begin{bmatrix} \dot{z}^\circ \\ \dot{\bar{z}} \end{bmatrix} = - \begin{bmatrix} 0 \\ \overline{H}^T \end{bmatrix} (J_v(\overline{H}\bar{z}))^T (v(\overline{H}\bar{z}) - d). \tag{14}$$

If we define $\overline{\phi}(\bar{z}) := \frac{1}{2}\|v(\overline{H}\bar{z}) - d\|^2$ then $\dot{\bar{z}} = -(\nabla\overline{\phi}(\bar{z}))^T$, and so \bar{z} is again a gradient system.

4.4 Existence and Uniqueness of Solutions

Using the coordinate transformation of the previous section it is possible to confirm existence and uniqueness of solutions in the (z°, \bar{z}) coordinates. The z° dynamics and the \bar{z} dynamics are decoupled, so we can analyze solutions independently. From Lemma 4.1 we know that $\dot{z}^\circ = 0$ so solutions trivially exist for all time. The dynamics of \bar{z} evolve according to a gradient system with potential function $\overline{\phi}(\bar{z})$, a radially unbounded function. Consider the sublevel set

$$\mathcal{U}_a := \{ \bar{z} \in \mathbb{R}^{2n-2} \mid \overline{\phi}(\bar{z}) \leq a \}$$

and define a Lyapunov function to be $V(\bar{z}) := \overline{\phi}(\bar{z})$. Denote by $-L_{\nabla\overline{\phi}}V(\bar{z})$ the Lie derivative of $-\nabla\overline{\phi}(\bar{z})^T$. For the \bar{z} system $-L_{\nabla\overline{\phi}}V(\bar{z}) = -\|\nabla\overline{\phi}(\bar{z})\|^2$, a negative semidefinite function. So the set \mathcal{U}_a is invariant for any $a > 0$. Furthermore, on the set \mathcal{U}_a , the function $\nabla\overline{\phi}(\bar{z})$ is Lipschitz continuous. Therefore, solutions $\bar{z}(t)$ exist for all time and are unique, for all initial conditions starting in \mathcal{U}_a .

4.5 Simulations

In this section we simulate the control law (8) for two graphs to gain some intuitive understanding about the controller's behaviour.

Example 4.2 Consider the complete graph K_4 with the rigidity function

$$g(z) = \begin{bmatrix} \|z_1 - z_2\|^2 \\ \|z_2 - z_3\|^2 \\ \|z_3 - z_4\|^2 \\ \|z_4 - z_1\|^2 \\ \|z_3 - z_1\|^2 \\ \|z_4 - z_2\|^2 \end{bmatrix} \text{ and } d = \begin{bmatrix} 1 \\ 2^2 \\ 1 \\ 2^2 \\ 5 \\ 5 \end{bmatrix}.$$

This graph is globally rigid and a point p in $g^{-1}(d)$ forms a rectangle with side lengths 1 and 2. Figure 5(a) shows the robots achieve the rectangle formation under the control (8). Figure 5(b) is for a different initial condition and here the final formation is a "twisted" rectangle; this equilibrium is not in $g^{-1}(d)$. Also, if the robots are initialized on a collinear configuration, then

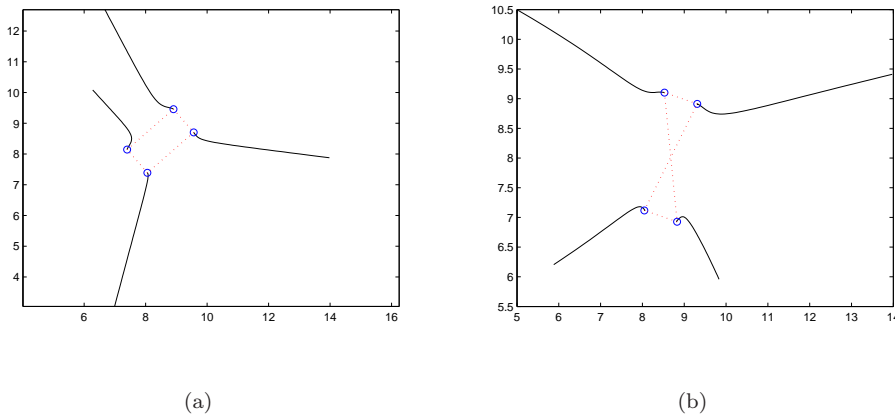


Figure 5. Four robots converge to an equilibrium that is a target formation and an equilibrium that is not a target formation.

they remain collinear; the collinear set is invariant and stable collinear equilibria exist. We conclude that the control (8) produces equilibria other than the target formation, so the set $g^{-1}(d)$ is not globally attractive. However, simulations suggest that it may be locally stable.

Example 4.3 Consider the control law derived from the minimally rigid graph G with four vertices with g and d given in (1). This graph has one fewer edge than the one used in the previous example. Additionally, if we remove any edge the graph will no longer be a rigid graph. Since G is a subgraph of K_4 , the target set in Example 4.2 is a subset of the target set in this example. This is confirmed in simulation. Although we have introduced additional equilibria in $g_G^{-1}(d)$, no twisted or undesired equilibrium has been found in simulation—other than the collinear equilibria. We conjecture that this may be because the minimally rigid framework leads to fewer terms in the control law; thus, there is less likelihood for terms in the control law to cancel each other to generate undesired equilibria.

5 Stability Results

In this section we present our main stability result. First, we identify several equilibrium sets associated with the formation control problem and we expose important properties of the desired set of equilibria, called \mathcal{E}_1 . Then, we linearize the dynamics (8) and, using infinitesimal rigidity of the formation graph, determine the eigenvalues of the linearized dynamics. Finally, we use center manifold theory to show that the set \mathcal{E}_1 is locally asymptotically stable. We conclude the section by comparing with several other proof techniques. To begin, the following assumption is crucial to our approach.

Assumption 5.1 Given a target formation $\{G, d\}$, we assume that $g_G^{-1}(d) \neq \emptyset$ and the framework (G, p) is infinitesimally rigid at each $p \in g_G^{-1}(d)$.

5.1 Equilibria

We are interested in studying the equilibria of (8). First we have the equilibrium set $\mathcal{E}_1 = g^{-1}(d)$, which represents the desired formations as specified by the formation graph:

$$\mathcal{E}_1 := \{z \mid g(z) - d = 0\} \equiv \{z \mid \phi(z) = 0\}.$$

Unfortunately, these are not the only equilibria of (8). There is also a larger set of equilibria

$$\mathcal{E}_2 := \{z \mid J_v(\hat{H}z)^T(g(z) - d) = 0 \}.$$

The matrix

$$J_v(\hat{H}z)^T = 2 \begin{bmatrix} e_1 & \dots & 0 \\ \vdots & \ddots & \vdots \\ \dots & e_m \end{bmatrix}$$

has a nontrivial kernel if and only if some $e_i = 0$, that is, two robots are collocated. So for a point z to be an equilibrium in \mathcal{E}_2 , for all i , $\|e_i\|^2 = d_i$ or $\|e_i\|^2 = 0$. Finally the complete set of equilibria of (8) is

$$\mathcal{E} = \{z \mid \nabla\phi(z) = 0 \}.$$

Notice that $\mathcal{E}_1 \subset \mathcal{E}_2 \subset \mathcal{E}$. Simulation has shown that, in general, $\mathcal{E}_2 \neq \mathcal{E}$. These extra equilibria are not unexpected: The matrix \hat{H}^T is $2n \times 2m$, so if $m > n$, then \hat{H}^T has a nontrivial kernel. In particular, the set \mathcal{E} includes equilibria where the robots are collinear.

It is also possible to define equilibrium sets for the reduced state \bar{z} . In particular, the desired target formations are

$$\bar{\mathcal{E}}_1 = \{ \bar{z} \in \mathbb{R}^{2N-2} \mid v(\bar{H}\bar{z}) = d \}.$$

The advantage of using $\bar{\mathcal{E}}_1$ rather than \mathcal{E}_1 in the ensuing stability analysis is that (it is easily shown that) $\bar{\mathcal{E}}_1$ is compact, whereas \mathcal{E}_1 is not.

To conclude this section, we examine some of the algebraic and geometric properties of $\mathcal{E}_1 = g^{-1}(d)$. First, observe that \mathcal{E}_1 is a real algebraic variety, since it is the intersection of the zero level sets of polynomial functions. This implies it has a finite number of connected components Whitney (1957). Under Assumption 5.1, \mathcal{E}_1 inherits further properties summarized in the following lemma.

Lemma 5.2: *If Assumption 5.1 holds, a set $\mathcal{S} \subset g^{-1}(d)$ is a topologically connected component of $g^{-1}(d)$ if and only if for each $p, p' \in g^{-1}(d)$, p and p' are related by a combination of rotations and translations of \mathbb{R}^2 , and \mathcal{S} is maximal with respect to rotations and translations. Moreover, \mathcal{E}_1 is a three dimensional embedded submanifold of \mathbb{R}^{2n} .*

Proof For the first statement, if G is globally rigid, then the result is immediately true because we know for all $p \in g^{-1}(d)$, $g^{-1}(d) = g_K^{-1}(g_K(p))$, where K is the complete graph associated with G , and the connected components of $g_K^{-1}(g_K(p))$ are generated by translations and rotations in the plane Asimow and Roth (1978). If G is not globally rigid, then $g^{-1}(d)$ contains additional points corresponding to parts of G being reflected. But if the points in p are not collinear—as they must be for G to be infinitesimally rigid—then any reflection in the plane of part of G at p corresponds to an embedding that is not in the same component of $g^{-1}(d)$ as p . Therefore, the property that points in a connected component of $g^{-1}(d)$ are generated only by translations and rotations in the plane is preserved.

For the proof of the second statement, if there are $2n - 3$ edges in the graph, then since $\text{rank} J_g(p) = 2n - 3$ for all $p \in g^{-1}(d)$, the result is an immediate application of the Preimage theorem (Boothby (1986), p. 80). However, if $m > 2n - 3$, a slightly more subtle argument is needed.

Fix $p \in g^{-1}(d)$ and suppose, without loss of generality, that $\hat{g} := (g_1, \dots, g_{2n-3})$, the first $2n - 3$ components of g , satisfy $\text{rank} J_{\hat{g}}(p) = 2n - 3$. Let \hat{G} denote the reduced graph with edges corresponding to \hat{g} . Denote by \mathcal{M}_p the maximal set of points related by a combination of

rotations and translations to p . A simple calculation shows that $J_{\hat{g}}(q)$ and $J_{\hat{g}}(p)$ are related by an invertible matrix when $q \in \mathcal{M}_p$. So $\text{rank } J_{\hat{g}}(q) = 2n - 3$ for all $q \in \mathcal{M}_p$. This implies that (\hat{G}, q) is infinitesimally rigid, and therefore rigid, for all $q \in \mathcal{M}_p$. Thus, there exists an open neighborhood \mathcal{U}_q of q such that $\mathcal{M}_p \cap \mathcal{U}_q = \hat{g}^{-1}(\hat{g}(p)) \cap \mathcal{U}_q$. Let $\mathcal{U} := \cup_{q \in \mathcal{M}_p} \mathcal{U}_q$, a $2n$ -dimensional manifold, be an open cover of \mathcal{M}_p . Then $\mathcal{M}_p \cap \mathcal{U} = \hat{g}^{-1}(\hat{g}(p)) \cap \mathcal{U}$. Thus, we have that $\hat{g} : \mathcal{U} \rightarrow \mathbb{R}^{2n-3}$ has rank $2n - 3$ for all $q \in \mathcal{M}_p$. Again by the Preimage theorem we obtain that \mathcal{M}_p is a 3-dimensional embedded submanifold of $\mathcal{U} \subset \mathbb{R}^{2n}$. In addition, from the first statement of the lemma, we know that \mathcal{M}_p is also a connected component of $g^{-1}(d)$. Thus, the result follows. \square

Remark 1: On a first reading, the infinitesimal rigidity condition in Assumption 5.1 seems difficult to check, since \mathcal{E}_1 is not compact. However, only a finite number of calculations must be made. It is easily verified that g is invariant under rigid body motions; that is, $g(z) = g(\hat{R}(z + \mathbf{1} \otimes w))$ where $w \in \mathbb{R}^2$, $R \in \mathbb{R}^{2 \times 2}$ is a rotation matrix and $\hat{R} = I_n \otimes R$. Therefore the Jacobian of $g(z)$ has constant rank on the components of \mathcal{E}_1 , so we must check the rank of the rigidity matrix at only one point on each component of \mathcal{E}_1 , or on one possible embedding. This is a finite test.

5.2 Linearized Dynamics

In order to study the stability of the equilibrium manifold \mathcal{E}_1 , we will consider the linearized z -dynamics on \mathcal{E}_1 .

Theorem 5.3: *The matrix $J_f(z)$ evaluated at a point on \mathcal{E}_1 has three zero eigenvalues; the rest are real and negative.*

Proof Let $z_0 \in \mathcal{E}_1$ and define $e_0 = \hat{H}z_0$. Also, let $f(z) = -J_g(z)^T(g(z) - d)$, the vector field for the z dynamics. Applying the product rule to f and using the fact that $g(z_0) - d = 0$ it follows that

$$J_f(z_0) = -J_g(z_0)^T J_g(z_0). \tag{15}$$

The matrix $J_f(z_0)$ is symmetric and thus has real eigenvalues, and also $\text{Ker}(J_f(z_0)) = \text{Ker}(J_g(z_0))$. The function $g(z)$ is the rigidity function for graph G and $J_g(z)$ is the rigidity matrix, so by Assumption 5.1, the rank of $J_g(z)$ is $2n - 3$ at all points on \mathcal{E}_1 . Therefore, $\dim(\text{Ker}J_g(z_0)) = 3$, so $J_f(z_0)$ has three zero eigenvalues. Moreover, the structure of $J_f(z_0)$ implies that it is a negative semidefinite matrix, so the non-zero eigenvalues are negative. \square

The previous results can also be extended to the reduced system $\dot{\bar{z}} = -(\nabla \bar{\phi}(\bar{z}))^T$. Let

$$\bar{f}(\bar{z}) := -\bar{H}^T (J_v(\bar{H}\bar{z}))^T (v(\bar{H}\bar{z}) - d).$$

Also define the function $\bar{g} : \mathbb{R}^{2n-2} \rightarrow \mathbb{R}^m$ by

$$\bar{g}(\bar{z}) := v(\bar{H}\bar{z}).$$

Corollary 5.4: *The matrix $J_{\bar{f}}(\bar{z})$ evaluated at a point on $\bar{\mathcal{E}}_1$ has one zero eigenvalue; the rest are real and negative.*

Proof First, analogous to the arguments above, we obtain that for $\bar{z}_0 \in \bar{\mathcal{E}}_1$

$$J_{\bar{f}}(\bar{z}_0) = -J_{\bar{g}}(\bar{z}_0)^T J_{\bar{g}}(\bar{z}_0).$$

Now we show that $J_{\bar{f}}(\bar{z}_0)$ has one zero eigenvalue and the remaining eigenvalues are stable. If

we linearize the (z°, \bar{z}) dynamics at a point $(z_0^\circ, \bar{z}_0) = Pz_0$ on \mathcal{E}_1 we obtain

$$\begin{bmatrix} \delta \dot{z}^\circ \\ \delta \dot{\bar{z}} \end{bmatrix} = \begin{bmatrix} 0 & 0 \\ 0 & J_{\mathcal{F}}(\bar{z}_0) \end{bmatrix} \begin{bmatrix} \delta z^\circ \\ \delta \bar{z} \end{bmatrix}.$$

Since PJ_fP^{-1} and $J_f(z_0)$ have the same eigenvalues, we know two zero eigenvalues correspond to the first two rows of PJ_fP^{-1} , while, by Theorem 5.3, the eigenvalues in the remaining block $J_{\mathcal{F}}(\bar{z}_0)$ are all stable except for one zero eigenvalue. □

5.3 Main Result

In this section we present our main result concerning asymptotic stability of the set \mathcal{E}_1 . This requires some background on set stability and on center manifold theory Carr (1981), which is our main tool for proving stability. After presenting the main result we discuss alternative proof approaches.

Let $\mathcal{S} \subset \mathbb{R}^\nu$ be a set and $x \in \mathbb{R}^\nu$ a point. Then the point to set distance is $\text{dist}(x, \mathcal{S}) = \inf_{y \in \mathcal{S}} \|x - y\|$. With respect to a dynamical system with state x we say a set \mathcal{S} is *stable* if

$$(\forall \epsilon > 0)(\exists \delta > 0) \text{dist}(x(0), \mathcal{S}) < \delta \Rightarrow (\forall t \geq 0) \text{dist}(x(t), \mathcal{S}) < \epsilon.$$

We say a set \mathcal{S} is *locally asymptotically stable* if it is stable and if

$$(\exists \delta > 0) \text{dist}(x(0), \mathcal{S}) < \delta \Rightarrow \lim_{t \rightarrow \infty} \text{dist}(x(t), \mathcal{S}) = 0.$$

Next we review center manifold theory. Consider a system in normal form

$$\dot{\theta} = A\theta + f_1(\theta, \rho) \tag{16}$$

$$\dot{\rho} = B\rho + f_2(\theta, \rho), \tag{17}$$

where $\theta \in \mathbb{R}^{\nu-\kappa}$, $\rho \in \mathbb{R}^\kappa$, A has eigenvalues only on the imaginary axis, B is Hurwitz, $f_1(0, 0) = 0$ and $f_2(0, 0) = 0$. The C^∞ functions f_1 and f_2 are restricted in order such that $J_{f_1}(0, 0) = 0$ and $J_{f_2}(0, 0) = 0$. An invariant manifold \mathcal{M} is a *center manifold* of (16)-(17) if it can be locally represented as

$$\mathcal{M} := \{ (\theta, \rho) \in \mathcal{U} \mid \rho = h(\theta) \}$$

where \mathcal{U} is a sufficiently small neighbourhood of the origin, $h(0) = 0$, and $J_h(0) = 0$. It can be shown that a center manifold always exists Carr (1981) and the dynamics of (16)-(17) restricted to the center manifold are

$$\dot{\xi} = A\xi + f_1(\xi, h(\xi)) \tag{18}$$

for a sufficiently small $\xi \in \mathbb{R}^{\nu-\kappa}$. The stability of the system (16)-(17) can then be analyzed from the dynamics on the center manifold using the next theorem.

Theorem 5.5: (Wiggins (1990), p. 195) *If the origin is stable under (18), then the origin of (16)-(17) is also stable. Moreover there exists a neighbourhood \mathcal{W} of the origin such that for*

every $(\theta(0), \rho(0)) \in \mathcal{W}$ there is a solution $\xi(t)$ of (18) and constants $c_i > 0$, $\gamma > 0$ such that

$$\begin{aligned}\theta(t) &= \xi(t) + r_1(t) \\ \rho(t) &= h(\xi(t)) + r_2(t),\end{aligned}$$

where $\|r_i(t)\| < c_i e^{-\gamma t}$.

The following is our main result.

Theorem 5.6: (Main Result) *Suppose Assumption 5.1 holds. Then \mathcal{E}_1 is locally asymptotically stable. Moreover, there exists a neighborhood \mathcal{U} of \mathcal{E}_1 such that for each $z(0) \in \mathcal{U}$ there exists a point $p \in \mathcal{E}_1$ where*

$$\lim_{t \rightarrow \infty} z(t) = p.$$

Proof To prove \mathcal{E}_1 is stable we study the (z°, \bar{z}) dynamics. First apply the linear transformation $P \in \mathbb{R}^{2n \times 2n}$ of Section 4.3 to separate the system into (z°, \bar{z}) components. The z° dynamics are stationary, so we study only the reduced \bar{z} system. Without loss of generality assume $\bar{z}_0 = 0$. From Corollary 5.4 and the symmetry of $J_{\bar{f}}(0)$ we know there exists an orthonormal transformation $Q \in \mathbb{R}^{(2n-2) \times (2n-2)}$ such that $QJ_{\bar{f}}(0)Q^T$ is in block diagonal form with a zero for the first term and a block $B \in \mathbb{R}^{(2n-3) \times (2n-3)}$ that is Hurwitz. Then rewrite the \bar{z} dynamics near $0 \in \bar{\mathcal{E}}_1$ as

$$\dot{\bar{z}} = J_{\bar{f}}(0)\bar{z} + (\bar{f}(\bar{z}) - J_{\bar{f}}(0)\bar{z}).$$

and define $(\theta, \rho) = Q\bar{z}$. Then it is easily verified that the (θ, ρ) dynamics have the form

$$\dot{\theta} = f_1(\theta, \rho) \tag{19}$$

$$\dot{\rho} = B\rho + f_2(\theta, \rho), \tag{20}$$

where $f_1(0, 0) = 0$ and $f_2(0, 0) = 0$, and $J_{f_1}(0, 0) = 0$ and $J_{f_2}(0, 0) = 0$.

Now we claim that $\mathcal{M} := \{(\theta, \rho) \mid (\exists \bar{z} \in \bar{\mathcal{E}}_1) (\theta, \rho) = Q\bar{z}\}$ is a center manifold for the system (19)-(20). First, \mathcal{M} is invariant because it consists of equilibria of (19)-(20). Second it is tangent to the θ -axis at 0. This can be seen as follows. Let

$$\tilde{g}(\theta, \rho) := \bar{g} \left(Q^T \begin{bmatrix} \theta \\ \rho \end{bmatrix} \right).$$

Then $\mathcal{M} = \{(\theta, \rho) \mid \tilde{g}(\theta, \rho) - d = 0\}$. We must show that the row vectors $\{d\tilde{g}_1(0), \dots, d\tilde{g}_m(0)\}$ that span the normal space of \mathcal{M} at 0, have their first entry equal to zero. Now observe that

$$\begin{bmatrix} d\tilde{g}_1(0) \\ \vdots \\ d\tilde{g}_m(0) \end{bmatrix} = J_{\bar{g}}(0)Q^T,$$

so we must show that the first column of $J_{\bar{g}}(0)Q^T$ is zero. But this follows from the fact that the first entry of $QJ_{\bar{f}}(0)Q^T = -(J_{\bar{g}}(0)Q^T)^T(J_{\bar{g}}(0)Q^T)$ is zero. Thus, there exists a function $h(\theta)$ such that in a neighborhood \mathcal{W}_0 of 0

$$\mathcal{M} \cap \mathcal{W}_0 = \{(\theta, \rho) \mid \rho = h(\theta)\}.$$

Since \mathcal{M} is an equilibrium manifold, we know that $f_1(\theta, h(\theta)) = 0$ on \mathcal{W}_0 . It follows that the dynamics restricted to \mathcal{M} are $\dot{\xi} = 0$, and thus $\xi(t) = \xi(0)$.

Now applying Theorem 5.5, we obtain the solutions for (θ, ρ) starting in \mathcal{W}_0 are

$$\begin{aligned}\theta(t) &= \xi(0) + r_1(t) \\ \rho(t) &= h(\xi(0)) + r_2(t),\end{aligned}$$

where $\|r_i(t)\| < c_i e^{-\gamma t}$ for some $c_1, c_2, \gamma > 0$. This implies $\lim_{t \rightarrow \infty} (\theta(t), \rho(t)) = (\xi(0), h(\xi(0))) \in \mathcal{M}$, so $\lim_{t \rightarrow \infty} \bar{z}(t) = Q^T(\xi(0), h(\xi(0))) \in \bar{\mathcal{E}}_1$, and $\lim_{t \rightarrow \infty} z(t) = P^{-1}(z^\circ(0), Q^T(\xi(0), h(\xi(0)))) \in \mathcal{E}_1$, as desired.

This argument can be repeated for each point on $\bar{\mathcal{E}}_1$ to obtain a cover $\{\mathcal{W}_k\}$ of $\bar{\mathcal{E}}_1$. Since $\bar{\mathcal{E}}_1$ is compact, we pass to a finite subcover to form a neighborhood of $\bar{\mathcal{E}}_1$. Local asymptotic stability of $\bar{\mathcal{E}}_1$ then follows. Finally, this argument can be trivially lifted to \mathcal{E}_1 since the center of mass dynamics are stationary. \square

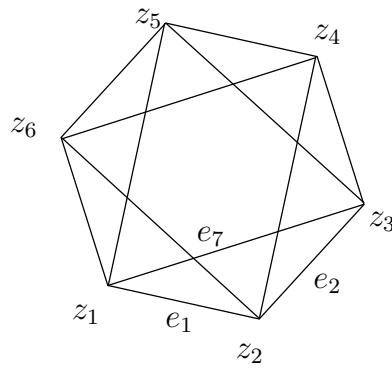
In summary, the infinitesimal rigidity of the formation graph was the key assumption in proving that the target set is an embedded submanifold and that the linearized dynamics have the required structure to apply center manifold theory. The local stability of the formation implies that if the robots experience small perturbations away from an equilibrium formation they will converge back to another nearby equilibrium point in the target set.

Remark 2: The proof approach of Olfati-Saber and Murray (2002) is to quotient out the dynamics on the equilibrium manifold so the equilibrium is topologically equivalent to a point. Suppose we have a system $\dot{x} = f(x)$ where $x \in \mathbb{R}^n$ and \mathcal{E} is an $(n - k)$ -dimensional manifold of equilibrium solutions. Quotienting out the dynamics on the manifold is equivalent to asking if there exists a diffeomorphism $\varphi : \mathbb{R}^n \rightarrow \mathbb{R}^{n-k} \times \mathbb{R}^k$ such that

$$\begin{aligned}\dot{\theta} &= f_1(\theta, \rho) \\ \dot{\rho} &= f_2(\rho),\end{aligned}$$

where $(\theta, \rho) = \varphi(x)$, $\left. \frac{\partial f_1}{\partial \theta} \right|_{\theta=0} = 0$ and $\mathcal{E} = \{ x \in \mathbb{R}^n \mid x = \varphi^{-1}(\theta, 0) \}$. If such a normal form exists then the stability of the equilibrium set becomes a study of the stability of $\rho = 0$. There are several difficulties in this approach. First, the change of coordinates must be global on the manifold \mathcal{E} . More importantly, it is not known if such a diffeomorphism exists for the formation problem (it was not derived in Olfati-Saber and Murray (2002)), and it can be computationally difficult to show $\left. \frac{\partial f_1}{\partial \theta} \right|_{\theta=0} = 0$. A few examples of this type of analysis for multi-agent systems exist in the literature (Marshall et al. (2006), p. 8), but they are rare due to the complexity of the computations.

Remark 3: It is possible to obtain the main result by other proof approaches. One approach is via Malkin's theorem (Malkin 1958), which provides the same result using standard Lyapunov arguments. However, Malkin's theorem requires that the system be placed in a normal form that is more difficult to obtain than the normal form for center manifold theory. In addition, Malkin's theorem is itself a special case of center manifold theory and indeed can be proved using center manifold theory (Sundarapandian 2003). LaSalle's theorem (Theorem 4.4, p. 128 in Khalil (2002)) can also be used to obtain a stability result, with the advantage that it does not require an eigenvalue analysis. However, it has several disadvantages. First, one must find a suitable Lyapunov function (this is not difficult in our case since ϕ is an obvious choice). Second, to conclude stability of \mathcal{E}_1 it must be proved that \mathcal{E}_1 is isolated from all other equilibrium sets. One way to do this is to exploit properties of gradient systems (Łojawiewicz 1959). Third, and most importantly, LaSalle's theorem gives no information about the behavior of trajectories as they approach \mathcal{E}_1 . In particular, it cannot be concluded that trajectories converge to a point on \mathcal{E}_1 . In summary, center manifold theory is the most concise and elegant way to obtain our result.

Figure 6. The graph G_6^* .

6 Regular Polygon Formations

An application of the formation stabilization control developed in the previous sections is to stabilize the robots to a regular polygon. A regular polygon is a useful formation for forming a large aperture antenna array.

We must first design a formation graph with a corresponding framework that is infinitesimally rigid. We can use the procedure outlined in Section 2.3.3 to build this graph, but there are other possible graphs. In particular, we are interested in graphs that result in *cyclically homogeneous* controls. Cyclical homogeneity is a type of symmetry in the control law such that when the indices 1 to n undergo a cyclic permutation, the control law is permuted by the same permutation. An example of cyclically homogeneous control laws is cyclic pursuit: $u_1 = z_2 - z_1, \dots, u_n = z_1 - z_n$. Cyclically homogeneous controls are desirable because an identical controller on each robot makes implementation easier. For our two dimensional robots the cyclic homogeneity property can be stated precisely in the following way: we define the $2n \times 2n$ fundamental permutation matrix P^* whose first block row is

$$\begin{bmatrix} 0 & I_2 & 0 & 0 & \dots & 0 \end{bmatrix} .$$

Then for a closed-loop system of the form $\dot{x} = f(x)$, if it has the symmetry $f(P^*z) = P^*f(z)$ we say that f has the property of *cyclic homogeneity*.

Now consider a graph denoted G^* with n vertices and $2n$ edges, such that vertex i is connected to vertices $i + 1$, $i + 2$, $i - 1$ and $i - 2$. The graph G_6^* is shown in Figure 6. We order the edges in the graph so that the expanded incidence matrix $\hat{H} = H \otimes I_2 \in \mathbb{R}^{4n \times 2n}$ is

$$\hat{H} := \begin{bmatrix} I_{2n} - P^* \\ I_{2n} - (P^*)^2 \end{bmatrix} .$$

Note that

$$\hat{H} = \begin{bmatrix} I_{2n} \\ I_{2n} + P^* \end{bmatrix} (I_{2n} - P^*)$$

thus if $e = \hat{H}z$ then $[I_{2n} + P^* - I_{2n}]e = 0$. Thus the components of e have a special form with $e_{i+n} = e_i + e_{i+1}$ for $i = 1, \dots, n$. Let

$$d^* := \begin{bmatrix} c\mathbf{1} \\ c^*\mathbf{1} \end{bmatrix} ,$$

where $\sqrt{c} \in \mathbb{R}$ is the side length of the regular polygon and

$$c^* := 4c \cos^2 \frac{\pi}{n}.$$

We assume that $c \neq 0$. If p is a point where the robots form a regular polygon, then $g_{G^*}(p) = d^*$. By construction, $g_{G^*}^{-1}(d^*) \neq \emptyset$. Techniques from graph theory can be used to show that the framework (G^*, p) is globally rigid and therefore, the robots located at $p \in \mathbb{R}^{2n}$ form a regular polygon if and only if $p \in g_{G^*}^{-1}(d^*)$. Thus, the regular polygon formation is the only formation in the set \mathcal{E}_1 , with two distinct embeddings (up to translation and rotation), corresponding to reflections of each other. All that remains to be done to apply our theory is to check the rank of the rigidity matrix on \mathcal{E}_1 .

Lemma 6.1: *The framework (G^*, p) is infinitesimally rigid for all $p \in g_{G^*}^{-1}(d^*)$.*

Proof The rigidity matrix is $J_{g_{G^*}}(p) = J_v(e)\hat{H}$, with $e = \hat{H}p$. The graph G^* is connected, so from Lemma 2.1 we know that $\dim(\text{Ker}(\hat{H})) = 2$. The strategy of the proof is to show that $\text{Im}(\hat{H}) \cap \text{Ker}(J_v(e)) = 1$, from which it follows that

$$\text{rank}(J_{g_{G^*}}(p)) = 2n - \dim(\text{Ker}(\hat{H})) - \dim(\text{Im}(\hat{H}) \cap \text{Ker}(J_v(e))) = 2n - 3.$$

Without loss of generality, we consider the counterclockwise embedding of G^* . Let $\xi := (\xi_1, \dots, \xi_{2n}) \in \mathbb{R}^{4n}$, with $\xi_i \in \mathbb{R}^2$, be a vector of the form

$$\xi = (w, R w, R^2 w, \dots, R^{n-1} w, (I + R)w, R(I + R)w, \dots, R^{n-1}(I + R)w),$$

where $w \in \text{Ker}(e_1^T)$, and $R \in \mathbb{R}^{2 \times 2}$ is the rotation matrix by $2\pi/n$ radians. We claim that $\text{Ker}(J_v(e)) = \text{span}\{\xi\}$. Since $J_{g_{G^*}}(p)$ cannot have rank greater than $2n - 3$ the result immediately follows.

From the geometry of the regular polygon we have that

$$e_i = R^{i-1} e_1 \quad i = 1, \dots, n \tag{21}$$

$$e_{n+i} = R^{i-1}(I + R)e_1 \quad i = 1, \dots, n. \tag{22}$$

To show $\xi \in \text{Ker}(J_v(e))$, we must show $e_i^T \xi_i = 0$, $i = 1, \dots, 2n$. From (21) we have that $e_i^T \xi_i = (R^{i-1} e_1)^T (R^{i-1} w) = e_1^T w = 0$, for $i = 1, \dots, n$. From (22) we have that $e_{n+i}^T \xi_{n+i} = (R^{i-1}(I + R)e_1)^T (R^{i-1}(I + R)w) = 0$, for $i = 1, \dots, n$, as desired. Conversely, suppose $\eta \in \text{Ker}(J_v(e))$; that is, $e_i^T \eta_i = 0$, and $e_{n+i}^T \eta_{n+i} = 0$, for $i = 1, \dots, n$. But this immediately implies, from the geometry of the plane, that $\eta_i = R^{i-1} \eta_1$ and $\eta_{n+i} = R^{i-1}(I + R)\eta_1$, for $i = 1, \dots, n$, with $e_1^T \eta_1 = 0$, as desired. □

Since graph G^* forms an infinitesimally rigid framework at regular points our gradient control can be applied to stabilize a regular polygon. Figure 7 shows six robots converging to a regular polygon using this control. In simulation, only initial conditions in the colinear set \mathcal{C} have been found to converge to collinear equilibria.

7 Directed Graphs

A drawback to the control designed so far is that it relies on two-way communication: If robot i 's control uses the position of robot j , then robot j 's uses the position of robot i . This may make implementation difficult when using cameras with a limited field of view. A control based on a directed graph may be easier to implement and is currently an area of active research in

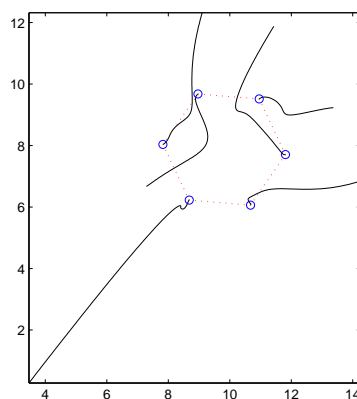


Figure 7. Six robots converging to a regular polygon.

the field of formation control (Hendrickx et al. 2006a). In this section we extend our procedure to the case of directed graphs.

7.1 Rigidity and Persistence

In this section we define rigidity and persistence in the context of directed graphs. Let G be a directed graph with n vertices. A *directed framework* for a directed graph is a pair (G, p) , where $p \in \mathbb{R}^{2n}$. Also denote by $g_G(p)$ the same rigidity function as before. Then the directed framework (G, p) is rigid if the corresponding undirected framework is rigid. Similarly, we define a directed framework (G, p) to be *infinitesimally rigid* if $\text{rank } J_{g_G}(p) = 2n - 3$. When using a directed graph to maintain a formation, it is not enough that the framework be rigid. There can be situations where some inter-robot distances are correct but it is impossible to satisfy the remaining distance constraints. If such a situation cannot happen, the graph is said to be *constraint consistent*. The precise definition of constraint consistency from Hendrickx et al. (2006a) is complex and beyond what is needed for the implementation proposed in this work. Instead, we will use the following sufficient condition from Hendrickx et al. (2006a).

Definition 7.1 A directed framework (G, p) is *constraint consistent* if each vertex has two or fewer outgoing edges.

Finally, a framework is *persistent* if it is both rigid and constraint consistent. A graph is *minimally persistent* if it is minimally rigid and constraint consistent.

Figure 8 shows why constraint consistency is needed in addition to rigidity when considering directed formations. Both graphs in Figure 8 are rigid: Figure 8(a) is also constraint consistent and thus persistent, whereas Figure 8(b) is not. If vertex 4 moves while still maintaining the distance to vertex 1 it is no longer possible for vertex 3 to maintain the lengths of its three outgoing edges.

The following useful theorem characterizes minimal persistence.

Theorem 7.2: (Theorem 4, Hendrickx et al. (2006a)) *A rigid graph is minimally persistent if and only if either*

- (1) *there are three vertices that have one outgoing edge, and the remaining vertices have two outgoing edges, or*
- (2) *there is one vertex that has no outgoing edge, one vertex that has one outgoing edge, and the remaining vertices have two outgoing edges.*

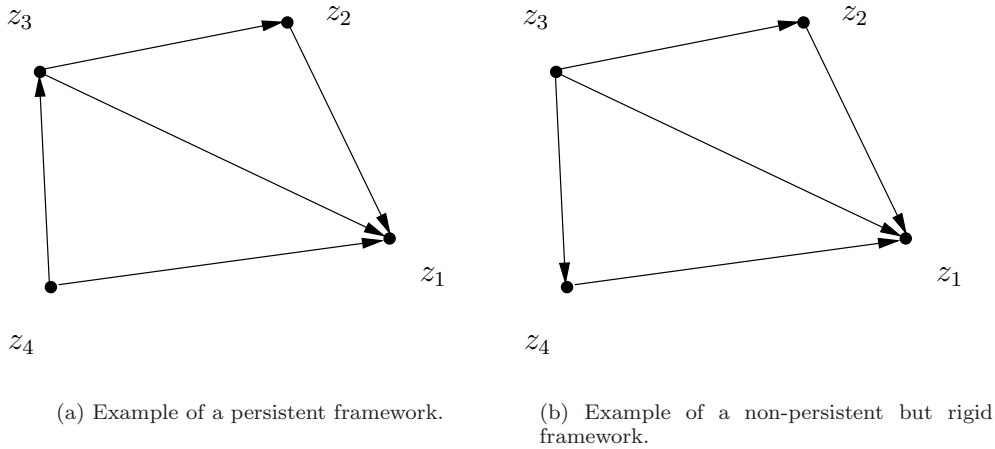


Figure 8. Two different rigid frameworks with four nodes.

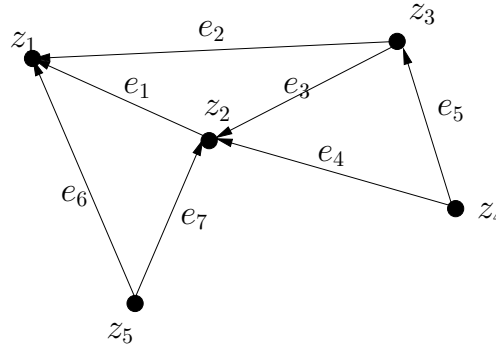


Figure 9. Graph created by recursively adding vertices in numerical order.

7.1.1 Constructing a Persistent Graph

To construct a persistent directed graph we use a modification of the Henneberg insertion technique described in Section 2.3.3. Let p be the location of the vertices in the plane. The first step is to add a directed edge from vertex 2 to vertex 1. All remaining vertices are connected to the graph in numerical order by creating two edges leaving from the vertex and going to two already added distinct vertices. Figure 9 shows a graph created using this procedure. Note that directed graphs formed by a sequence of Henneberg insertions are persistent and satisfy case 2 in Theorem 7.2.

7.2 Control Law

In this section we develop a control law for directed graphs. The primary modification is that instead of using a global potential function, each robot has its own potential function. Let $\phi_i(z)$ be the potential function for robot i . Also define $e := \hat{H}z$.

In Figure 9, robot 1 has no outgoing edges so define $\phi_1(z) := 0$. Robot 2 has only one outgoing edge, so let $\phi_2(z) := \frac{1}{2}(\|e_1\|^2 - d_1)^2$. All other robots have two outgoing edges. For robot $i > 2$ with outgoing edges e_j and e_k , define the potential function

$$\phi_i(z) := \frac{1}{2}(\|e_j\|^2 - d_j)^2 + \frac{1}{2}(\|e_k\|^2 - d_k)^2.$$

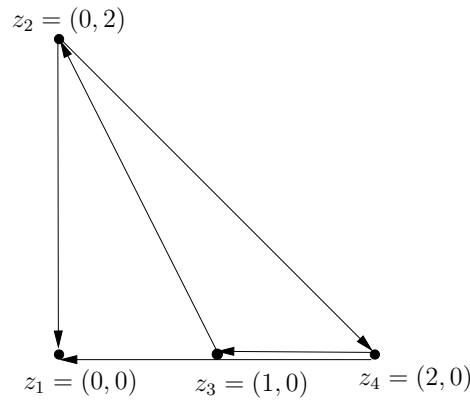


Figure 10. A directed graph that is infinitesimally rigid, but has a vertex (z_4) with two parallel outgoing edges.

The control law for each robot is then taken to be

$$u_i = -\frac{\partial}{\partial z_i} \phi_i(z)^T \tag{23}$$

so $\dot{z}_i = -\frac{\partial}{\partial z_i} \phi_i(z)^T$. Denote by $\dot{z} = f(z)$ the resulting closed-loop system.

7.3 Stability Analysis

Lemma 7.3: For each $p \in g_G^{-1}(d)$, $J_f(p)$ is block lower triangular.

The proof follows from the Henneberg insertion construction together with equation (10). For example, for Figure 9

$$J_f(p) = 4 \begin{bmatrix} 0 & 0 & 0 & 0 \cdots 0 \\ e_1 e_1^T & -e_1 e_1^T & 0 & 0 \cdots 0 \\ e_2 e_2^T & e_3 e_3^T & -e_2 e_2^T - e_3 e_3^T & 0 \cdots 0 \\ \vdots & & & \end{bmatrix}.$$

Theorem 7.4: Assume $p \in g_G^{-1}(d)$ and for each $i > 2$ the edges leaving vertex i are not collinear. Then $J_f(p)$ has three zero eigenvalues and the rest are real and negative.

Proof From Lemma 7.3 we know that the matrix $J_f(p)$ is block lower triangular. The first two rows of $J_f(p)$ are zero. Thus the first 2×2 block on the main diagonal has two zero eigenvalues. The second 2×2 block is $-e_1 e_1^T$, a negative semidefinite matrix with rank 1, and so has one zero eigenvalue and one negative real eigenvalue. Each subsequent 2×2 block on the main diagonal has the form $-e_j e_j^T - e_k e_k^T$ and is the sum of two negative semidefinite matrices, and thus is also a negative semidefinite matrix. By the non-collinearity assumption, edges e_j and e_k leaving vertex i are linearly independent, so the third block has rank 2 and thus has two negative real eigenvalues. \square

Remark 1: Instead of an infinitesimal rigidity condition on the graph as in Theorem 5.3, we have a non-collinearity condition on the edges leaving a graph. One may ask if the non-collinearity condition is implied by the infinitesimal rigidity condition. However, Figure 10 provides a counterexample, showing a graph may be infinitesimally rigid and have one vertex with two collinear edges leaving it.

The following theorem shows that the results of Section 5 can be extended to the special case of directed graphs constructed using Henneberg insertions.

Theorem 7.5: *Let G be a directed graph constructed using a sequence of Henneberg insertions. If, for each $p \in g_G^{-1}(d)$, G is infinitesimally rigid and no vertex has collinear outgoing edges, then \mathcal{E}_1 is locally asymptotically stable. Moreover, there exists a neighborhood \mathcal{U} of \mathcal{E}_1 such that for each $z(0) \in \mathcal{U}$ there exists a point $p \in \mathcal{E}_1$ such that $\lim_{t \rightarrow \infty} z(t) = p$.*

Proof The proof largely follows from the results of Section 5. First we separate the stationary z_1 dynamics from the rest of the system. Define

$$P_2 = \begin{bmatrix} I_2 & 0 & 0 & \dots & 0 \\ -I_2 & I_2 & 0 & \dots & 0 \\ -I_2 & 0 & I_2 & \dots & 0 \\ \vdots & \vdots & \ddots & \dots & \vdots \\ -I_2 & 0 & \dots & \dots & I_2 \end{bmatrix}.$$

and $(z_1, \psi) = P_2 z$. Thus $\psi = (z_2 - z_1, \dots, z_N - z_1)$. Note that if $e_i = z_j - z_1$, then $e_i = \psi_j$, and if $e_i = z_j - z_k$, then $e_i = \psi_j - \psi_k$. So it is possible to find a matrix M such that $e = M\psi$. Further define

$$\bar{\mathcal{E}}_1 := \{ \psi \in \mathbb{R}^{2N-2} \mid v(e) = v(M\psi) = d \}.$$

Note that $\mathcal{E}_1 = \mathbb{R}^2 \times \bar{\mathcal{E}}_1$. Additionally, we see that $\bar{\mathcal{E}}_1$ is compact and each component is diffeomorphic to S^1 . Define $\dot{\psi} = f_\psi(\psi)$ to be the closed-loop ψ dynamics. To prove \mathcal{E}_1 is stable we study these ψ dynamics. From the structure of $f(z)$ it is clear that $\bar{\mathcal{E}}_1$ is stable if and only if \mathcal{E}_1 is stable. In order to apply Theorem 5.6 it remains to show only that the Jacobian of the ψ dynamics meets the eigenvalue requirement. But this follows from Theorem 7.4 and arguments analogous to those in the proof of Corollary 5.4. \square

7.4 General Directed Graphs

If an arbitrary directed graph is used to derive the potential functions for each robot, the analysis of the linearized dynamics is not so simple. However, if the linearized dynamics have three zero eigenvalues and the rest have negative real parts it is still possible to apply Theorem 5.6 to conclude that the formation is stable. The following example has linearized dynamics that are not upper triangular, but by checking the eigenvalues numerically we can see that the results of Section 5 apply.

Example 7.6 Consider the framework in Figure 11. Let the location of the vertices be p . The graph is infinitesimally rigid, and thus \mathcal{E}_1 is an embedded submanifold.

If we linearize we see that for $z \in \mathcal{E}_1$

$$J_f(z) = 4 \begin{bmatrix} 0 & 0 & 0 & 0 \\ e_1 e_1^T & -e_1 e_1^T - e_2 e_2^T & e_2 e_2^T & 0 \\ e_3 e_3^T & 0 & -e_2 e_2^T - e_4 e_4^T & e_4 e_4^T \\ 0 & e_5 e_5^T & 0 & -e_5 e_5^T \end{bmatrix}.$$

Note that $J_f(z)$ is not block lower triangular, nor is there any way to permute the indices to make the matrix block lower triangular. The graph in Figure 11 could not have been created using the Henneberg insertion method. Hendrickx et al. (2006b) discusses other operations that can produce such a directed graph.) If we evaluate the eigenvalues of $J_f(z)$ numerically we see that there are three zero eigenvalues and the rest are real and stable. Thus, Theorem 5.6 applies and the formation is locally asymptotically stable. This example shows that the procedure in Section 7.1.1 to construct a directed graph to stabilize formations is sufficient but not necessary for stability.

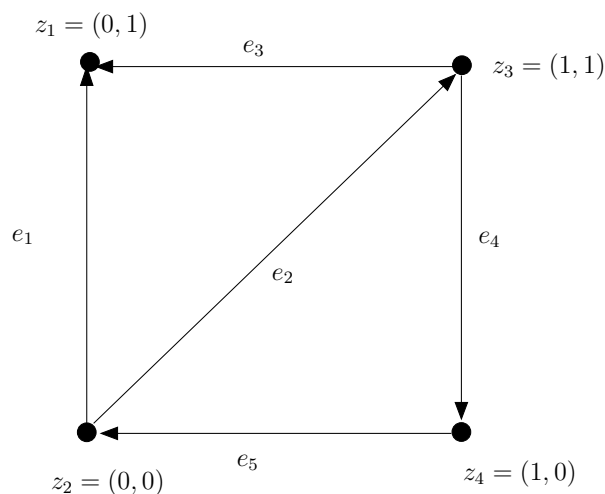


Figure 11. Due to the arrangement of the edges leaving vertex 3 this graph could not have been created using the Henneberg insertion procedure.

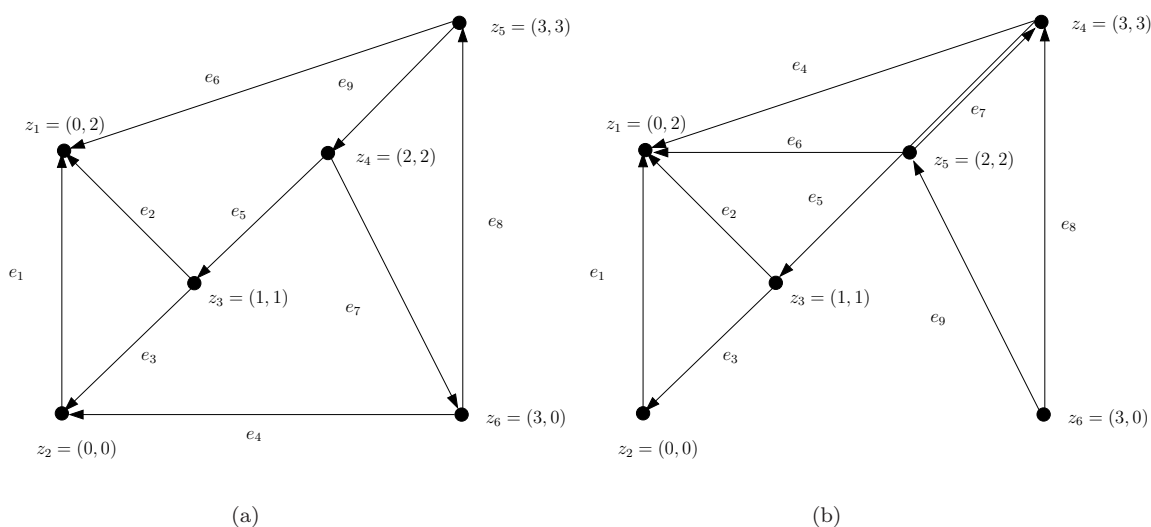


Figure 12. Embeddings of a directed graph for six robots.

Conversely, there are some directed graphs where we cannot apply our results. Related to Figure 12(a) $J_f(z)$ has 4 zero eigenvalues and the rest are real and stable. Thus the conditions to apply Theorem 5.6 do not hold as there are more zero eigenvalues than the dimension of the equilibrium manifold and we can make no conclusion about the stability of this formation using this analysis technique. It turns out that if we modify the graph as shown in Figure 12(b) (note that now there is no directed edge from z_5 to z_3), then there are three zero eigenvalues and the rest have negative real parts. Thus we can conclude that this formation is stable.

8 Conclusion

This paper considers the problem of stabilizing a group of robots to a desired target formation using decentralized control. The target formation is defined in terms of a set of inter-robot distances and we place the restriction that these distances correspond exactly to the sensor capabilities of each robot. A gradient control law based on a potential function derived from the target distances is proposed. Our results show that the crucial property to achieve local stability

is that the framework corresponding to the target formation be infinitesimally rigid. Under the assumption of infinitesimal rigidity, the set of equilibria of the gradient dynamics corresponding to the target formation becomes an embedded submanifold, and further, this submanifold is a center manifold. Thus, standard tools from center manifold theory are applied to obtain a local stability result. Next, we address the particular case of regular polygon formations where it is shown that the main assumption of infinitesimal rigidity holds for a suitable formation graph. A shortcoming of the approach is that it assumes two-way sensor capability of the robots. This drawback is overcome by extending the theory to the case of directed sensor graphs. It is shown that the main stability result extends to directed graphs when the target formation is constructed using a Henneberg insertion procedure. Examples are given to show when our theory does not apply to more general directed sensor graphs. An experimental validation of the proposed controller was carried out, though not described here, and details of those results can be found in Krick (2007).

Acknowledgements. The authors thank Manfredi Maggiore for a helpful discussion on center manifold theory.

References

- Marshall, J., Broucke, M., and Francis, B. (2004), “Formations of Vehicles in Cyclic Pursuit,” *IEEE Transactions on Automatic Control*, 9(11), 1963–1974.
- Cortés, J., Martínez, S., and Bullo, F. (2004), “Robust Rendezvous for Mobile Autonomous Agents via Proximity Graphs in d Dimensions,” *IEEE Transactions on Automatic Control*, 51(8), 1289–1298.
- Lin, J., Morse, A., and Anderson, B. (2004), “The Multi-Agent Rendezvous Problem - The Asynchronous Case,” in *Proceedings of the 43rd IEEE Conference on Decision and Control*, December, Vol. 2, Atlantis, Bahamas, pp. 1926–1931.
- Goldenberg, D., Lin, J., Morse, A., Rosen, B., and Yang, Y. (2004), “Towards Mobility As A Network Control Primitive,” in *Proceedings of the 5th ACM International Symposium on Mobile ad hoc Networking and Computing*, Tokyo, Japan, pp. 163–174.
- Cortés, J., Martínez, S., Karatas, T., and Bullo, F. (2004), “Coverage Control for Mobile Sensing Networks,” *IEEE Transactions on Robotics and Automation*, 2(2), 243–255.
- Olfati-Saber, R. (2006), “Flocking for multi-agent dynamic systems: Algorithms and theory,” *IEEE Transactions on Automatic Control*, 51, 401–420.
- Smith, S., Broucke, M., and Francis, B. (2006), “Stabilizing a Multi-Agent System to an Equilateral Polygon Formation,” in *Proceedings of the 17th International Symposium on Mathematical Theory of Networks and Systems (MTNS2006)*, Kyoto, Japan, pp. 2415–2424.
- Olfati-Saber, R., and Murray, R. (2002), “Distributed Cooperative Control of Multiple Vehicle Formations using Structural Potential Functions,” in *Proceedings of the 15th IFAC World Congress*, Barcelona, Spain.
- Biggs, N., *Algebraic Graph Theory*, Cambridge University Press (1974).
- Asimow, L., and Roth, B. (1979), “The Rigidity of Graphs II,” *Journal of Mathematical Analysis and Applications*, 68(1), 171–190.
- Bereg, S. (2005), “Certifying and Constructing Minimally Rigid Graphs in the Plane,” in *Proceedings of the Twenty-First Annual Symposium on Computational Geometry*, Pisa, Italy: Annual Symposium on Computational Geometry, pp. 73–80.
- Whitney, H. (1957), “Elementary Structure of Real Algebraic Varieties,” *The Annals of Mathematics*, 66(3), 545–556.
- Asimow, L., and Roth, B. (1978), “The Rigidity of Graphs,” *Transactions of the American Mathematical Society*, 245, 279–289.
- Boothby, W., *An Introduction to Differentiable Manifolds and Riemannian Geometry*, Academic Press Inc. (1986).
- Carr, J., *Applications of Centre Manifold Theory*, Springer-Verlag (1981).
- Wiggins, S., *Introduction to Applied Nonlinear Dynamical Systems and Chaos*, Springer-Verlag (1990).
- Marshall, J., Broucke, M., and Francis, B. (2006), “Pursuit Formations of Unicycles,” *Automatica*, 42(1), 3–12.

- Malkin, I., *Theory of Stability of Motion*, United States Atomic Energy Commission Technical Information Service (1958).
- Sundarapandian, V. (2003), “A Geometric Proof of Malkin’s Stability Theorem,” *Indian Journal of Pure and Applied Mathematics*, 34(7), 1085–1088.
- Khalil, H., *Nonlinear Systems*, Prentice Hall (2002).
- Lojawiewicz, S. (1959), “Sur le problème de la division,” *Studia Mathematica*, 18, 87–136.
- Hendrickx, J., Anderson, B., Delvenne, J.C., and Blondel, V. (2006a), “Directed Graphs for the Analysis of Rigidity and Persistence in Autonomous Agent Systems,” *International Journal of Robust and Nonlinear Control*, 17(10-11), 960–981.
- Hendrickx, J., Fidan, B., Changbin, Y., Anderson, B., and Blondel, V. (2006b), “Elementary Operations for the Reorganization of Minimally Persistent Formations,” in *Proceeds of the 17th International Symposium on Mathematical Theory of Networks and Systems (MTNS2006)*, June, Kyoto, Japan, pp. 859–873.
- Krick, L., “Application of Graph Rigidity in Formation Control of Multi-Robot Networks,” MSc Thesis, University of Toronto, Electrical and Computer Engineering Dept. (2007).